2018 IEEE 14th International Conference on Control and Automation (ICCA)
June 12-15, 2018. Anchorage, Alaska, USA

Trajectory-Tracking Sliding-Mode Control of the Autonomous Wheelchair Modeled as a Nonholonomic WMR

A. Filipescu, R. Solea, A. Filipescu Jr., G. Stamatescu, G. Ciubucciu

***Abstract*—This paper deals a new approach of the trajectory-tracking second-order sliding-mode control (TT-SOSMC), applied to control a nonholonomic wheelchair for elderly and disabled based on kinematic model. Cirrus Power Wheelchair (CPW) was modelled like a wheeled mobile robot (WMR) with two driving and two free wheels (2DW/2FW). A hardware description, concerning driving wheels control, data acquisition and communication with PC and touch screen, is presented. Simulations and real time results have presented taking into account parameter uncertainties and external disturbances. CPW closed loop control, via simulation and real-time have proved improved performance in terms of decreasing reaching and settling times with increasing robustness.**

I. Introduction

The progress in autonomy of the wheeled mobile robots made possible applications in various and useful fields like the use of intelligent powered wheelchairs to assist handicapped and elderly people with light and/or severe neuro-motor disabilities. Up to now, the research about autonomous wheelchair has incorporated classic solutions for low level control. Today, the research addresses high level control, [6]. The trajectory tracking control, which is one of basic navigation problems, means to track reference trajectories either a priori defined or given by path planners. Sliding mode control is a well-known control method which has been successfully and widely applied to systems with external bounded disturbance and parameter and/or model uncertainties, [1]. The reason for the popularity of this method is one of its most attractive features: its robustness to external disturbances, parameter variations and uncertainties [3], [4]. Unfortunately, the drawback of the SMC is the presence of chattering, due to the switching frequency of the control. The use of the high order sliding-mode controllers to alleviate or eliminate the chartering and to keep high robustness are the main advantages of the original approach of the SMC, [1], [2], [7] and [8]. The high order sliding-mode uses differentiators and sliding manifold estimators, [5], to maintain the robustness of the system. The second order sliding mode control, like as the super-twisting sliding mode control, is easy to implement in real-time, assuring robustness to uncertainties. This paper proposes a trajectory-tracking second-order sliding-mode controller based on WMR kinematic model, acquisition data from encoders, computing on embedded PC the control low and sent it to wheelchair.

The rest of the paper is organized as follows: Cirrus Power Wheelchair hardware, concerning driving wheels control, data acquisition and communication with PC and touch screen is presented in Section II; nonholonomic wheelchair kinematic model is laid out in Section III; wheelchair tracking errors dynamics are presented in Section IV; wheelchair first and second order sliding-mode control based on kinematic model are presented in Section V; Section VI is reserved to closed loop, real-time control of CPW; some final remarks can be found in Section VII.

II. Equipped CPW

The wheels are driven by brush DC motors. For controlling DC motors were used servo amplifier 50A8, shown in Fig.1. It can receive data from acquisition board and, based on the received signal, the servo-amplifier will send a PWM control signal to DC motor, signal having a duty cycle dynamically modifiable. For data acquisition and control signal sending to the DC motors has been a NI-6024 acquisition card, also shown in Fig. 1. It has 16 analogue inputs, two analogue outputs 8 digital inputs and 8 digital outputs. The communication between the motherboard and data acquisition card is a PCI slot. This device connects to PC the servo-amplifies, DC motors and the encoders (Fig. 1). PC processes signals and data necessary for odometer system implementation. Cirrus Power Wheelchair fully equipped with PC, data acquisition card, servo-amplifiers, DC motors, encoders and batteries is shown in Fig. 2.

III. Nonholonomic Wheelchair Kinematic Model

Fig. 3 shows a geometric model of a wheelchair that defines the main variables necessary to obtain kinematic model This WMR has two diametrically opposed drive wheels (radius r) and free-wheeling castors. Both drive

*This work was supported by a grant of the Romanian Ministry of Research and Innovation, CCCDI-UEFISCDI, project number, PN-III-P1-1.2-PCCDI-2017-0290.

Adrian Filipescu, Ph. D., Eng., is professor with the Department of Automation and Electrical Engineering, "Dunarea de Jos" University of Galati, Domneasca 47, 800008, Galati, Romania (Corresponding author, Phone: +40724537594; fax: +40 236 460182, e-mail: adrian.filipescu@ugal.ro)

Razvan. Solea, Ph. D., Eng., is associate professor with the Department of Automation and Electrical Engineering, "Dunarea de Jos" University of Galati, (e-mail: razvan.solea@ugal.ro).

Adriana Filipescu, Ph. D., Eng., is researcher with the Department of Automation and Electrical Engineering, "Dunarea de Jos" University of Galati, (e-mail: adriana.filipescu@ugal.ro).

Grigore Stamatescu, Ph. D., Eng., is assoc professor with the Department of Automation and Industrial Informatics, Polytechnic University of Bucharest (e-mail: grigore.stamatescu@upb.ro).

George Ciubucciu is Ph. D. student with the Department of Automation and Electrical Engineering, "Dunarea de Jos" University of Galati, Domneasca 47, 800008, Galati, Romania (Corresponding author, Phone: +40724537594; fax: +40 236 460182, (e-mail: ciubucciu.george@yahoo.com)

wheels are actuate and sensed, while the castors are neither actuated nor sensed. Thus, the castor wheels are not considered in getting of kinematic and dynamic models. P_o defines the origin of the robot coordinate system with coordinates (x_o, y_o). P_c is the centre of mass of the robot with coordinates (x_c, y_c) and is placed in the X-axis at a distance d of P_o. P_l is a virtual reference point attached to the platform with coordinates (x_l, y_l) and is placed in the X-axis at a distance L_h of P_c. L is the length of the axis between the wheels of the mobile robot. ϕ is the angle between x-axis of $\{W\}$ and the X-axis of $\{R\}$. $\dot{\delta}_R$ and $\dot{\delta}_L$ are the angular speeds of the right and left wheels around the Y-axis.

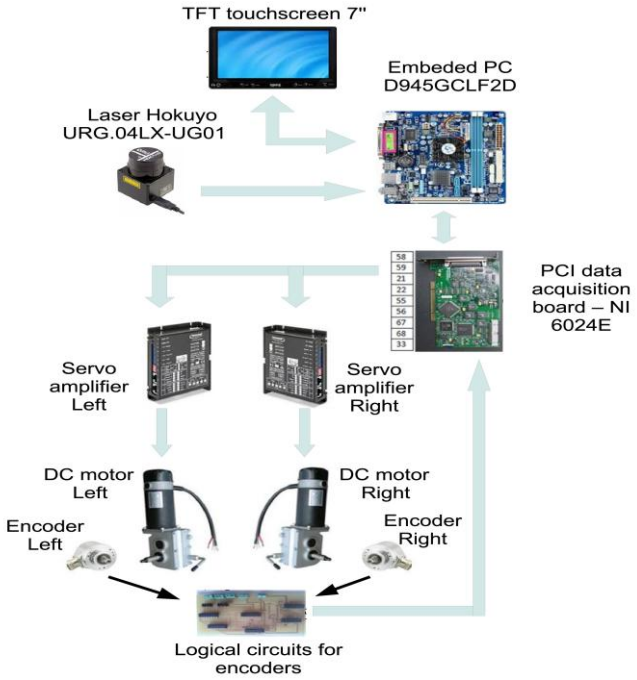

Figure 1. Control and navigation hardware

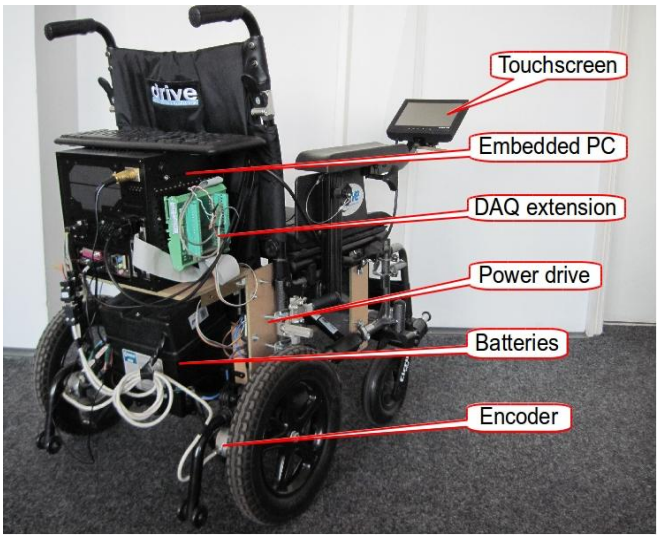

Figure 2. Equipped Cirrus Power Wheelchair

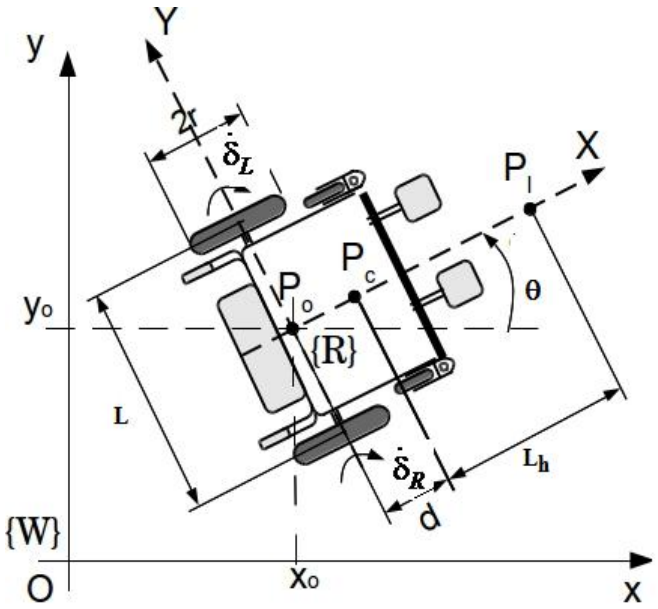

Figure 3. Wheelchair modelled as wheeled mobile robot with two driving wheels and two free wheels (2DW/2FW)

The equilibrium of the wheelchair is maintained by two front free wheels and other two rear small wheels, whose effect it will ignore. Thus,

$$q = [x_c \quad y_c \quad \theta \quad \delta_R \quad \delta_L] \tag{1}$$

denotes the configuration of the system, i.e. the five generalized coordinates $(n = 5)$. In the kinematic model it is suppose that in each contact exist a pure rolling motion. Assuming that the velocity of P_o must be in the direction of the symmetry (X-axis) and the wheels do not slip, the following constraints set $(m = 3)$, with respect to P_c, can be expressed, [6]:

$$\dot{y}_c \cos\theta - \dot{x}_c \sin\theta - \dot{\theta} d = 0 \tag{2}$$

$$\dot{x}_c \cos\theta + \dot{y}_c \sin\theta + \frac{L}{2}\dot{\theta} - r\dot{\delta}_R = 0 \tag{3}$$

$$\dot{x}_c \cos\theta + \dot{y}_c \sin\theta - \frac{L}{2}\dot{\theta} - r\dot{\delta}_L = 0 \tag{4}$$

These constraints can be rewritten in the matrix form:

$$A(q)\dot{q} = 0 \tag{5}$$

with

$$A(q) = \begin{bmatrix} -\sin\theta & \cos\theta & -d & 0 & 0 \\ -\cos\theta & -\sin\theta & -L/2 & r & 0 \\ -\cos\theta & -\sin\theta & L/2 & 0 & r \end{bmatrix} \tag{6}$$

Considering the wheelchair kinematics, the following equation is satisfied

$$A(q)S(q) = 0 \tag{7}$$

with

$$S(q)=\begin{bmatrix} c(\frac{L}{2}\cos\theta - d\sin\theta) & c(\frac{L}{2}\cos\theta + d\sin\theta) \\ c(\frac{L}{2}\sin\theta + d\cos\theta) & c(\frac{L}{2}\sin\theta - d\cos\theta) \\ c & -c \\ 1 & 0 \\ 0 & 1 \end{bmatrix} \quad (8)$$

where $c = r/L$. The kinematic model, is given by

$$\dot{q} = S(q)\delta(t) \quad (9)$$

with $\delta = [\delta_R \quad \delta_L]^T$

IV. TRACKING ERRORS

The simplified kinematic model of the wheelchair can be expressed as:

$$\begin{bmatrix} \dot{x}_r \\ \dot{y}_r \\ \dot{\theta}_r \end{bmatrix} = \begin{bmatrix} \cos(\theta_r) & 0 \\ \sin(\theta_r) & 0 \\ 0 & 1 \end{bmatrix} \begin{bmatrix} \upsilon_r \\ \omega_r \end{bmatrix} \quad (10)$$

where: x_r şi y_r are the Cartesian coordinates, υ_r is linear speed, θ_r is the orientation and ω_r is the angular speed of the real position of the wheelchair geometrical centre. Similar to (10), x_d and y_d are the Cartesian coordinates, υ_d is linear speed, θ_d is the orientation and ω_d is the angular speed of the desired position of the wheelchair geometrical centre.

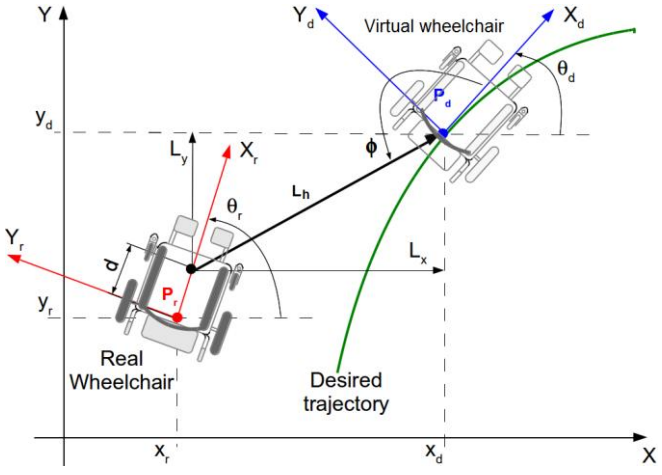

Figure 4. Real and desired wheelchair trajectories

When the controlled wheelchair tracks the desired trajectory, the following errors can be defined as follows, Fig. 4:

$$\begin{aligned} L_x &= x_d - x_r - d\cos(\theta_r) \\ L_y &= y_d - y_r - d\sin(\theta_r) \\ \theta_e &= \theta_d - \theta_r \end{aligned} \quad (11)$$

The distance L_h between the real and virtual wheelchair is measured from the centre of the two rear wheels of the virtual wheelchair to the front of the real wheelchair (offset by d from the centre of the two rear wheels in the axis). The attitude angle $\phi \in (-\pi \quad \pi]$ is measured from the line of orientation of the virtual wheelchair to the distance line between the two robots (real and virtual).

$$L_h^2 = L_x^2 + L_y^2 \quad (12)$$

$$\phi = \arctan 2(L_y, L_x) - \theta_d + \pi \quad (13)$$

$$\theta_e = \theta_d - \theta_r \quad (14)$$

By derivation (12), (13) and (14), the linear speed coordinates and the angular speed can be expressed as:

$$\begin{aligned} \dot{L}_x &= \upsilon_d\cos(\theta_d) - \upsilon_r\cos(\theta_r) + d\omega_r\sin(\theta_r) \\ \dot{L}_y &= \upsilon_d\sin(\theta_d) - \upsilon_r\sin(\theta_r) - d\omega_r\cos(\theta_r) \\ \dot{\theta}_e &= \omega_d - \omega_r \end{aligned} \quad (15)$$

Replacing (15) in the derivatives of (12) and (13), after some trigonometric manipulation, the derivative expressions of L_h , ϕ are:

$$\dot{L}_h = -\upsilon_d\cos(\phi) + \upsilon_r\cos(\gamma) + d\omega_r\sin(\gamma) \quad (16)$$

$$\dot{\phi} = L_h^{-1}[\upsilon_d\sin(\phi) - \upsilon_r\sin(\gamma) + d\omega_r\cos(\gamma) - L_h\omega_d] \quad (17)$$

The dynamics of the tracking error vector can be expressed as:

$$\dot{e} = A(e,t) + B(e,t)u \quad (18)$$

$$A(e,t) = \begin{bmatrix} -\upsilon_d\cos(\phi_e + \phi_d) \\ \dfrac{\upsilon_d\sin(\phi_e + \phi_d) - (L_{h_e} + L_{h_d})\omega_d}{L_{h_e} + L_{h_d}} \end{bmatrix} \quad (19)$$

$$B(e,t) = \begin{bmatrix} \cos(\gamma_e) & d\sin(\gamma_e) \\ \dfrac{-\sin(\gamma_e)}{L_{h_e} + L_{h_d}} & \dfrac{d\cos(\gamma_e)}{L_{h_e} + L_{h_d}} \end{bmatrix} \quad (20)$$

where: $\gamma = \theta_d - \theta_r + \phi$, $\gamma_e = \theta_e + \phi_e + \phi_d$, $\phi_e = \phi_d - \phi_r$, $L_{h_e} = L_h - L_{h_d}$, with $u = [\upsilon_r \quad \omega_r]^T$ the control input and $e = [L_{h_e} \quad \phi_e]^T$ the controlled output.

Because $L_h > 0$ and $d > 0$, the matrix B is non-singular, $\det(B) = d/(L_h)$, $\det(B) \neq 0$ and the control input can be computed.

V. FIRST AND SECOND ORDER TT-SMC OF THE CPW

The TT-SMC architecture of CPW like a WMR with 2DW/2FW is shown in Fig. 5. This driving architecture allows CPW to tracks a desired trajectory with a required speed profile. Trajectory tracking assumes that the CPW follows a virtual one that moves on the desired trajectory with the required speed profile, Fig.6 and Fig.7

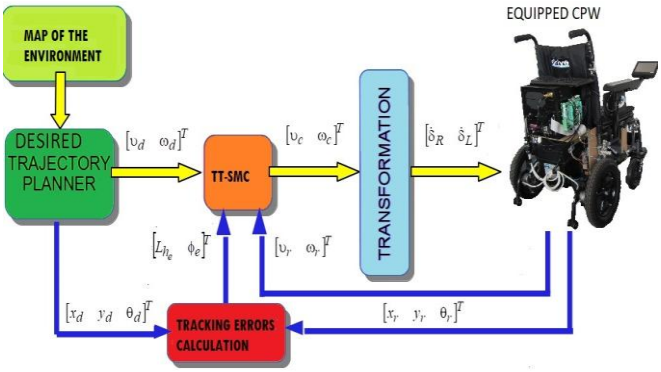

Figure 5. Closed-loop trajectory-tracking sliding-mode control of wheelchair

For the first order sliding-mode control (FOSMC), it chooses the following the reaching control input vector, [7], is defined as:

$$u_{fosm} = \begin{bmatrix} u_{fosm1} \\ u_{fosm2} \end{bmatrix} = -qsign(s) - ps, \qquad (21)$$
$$q > 0, \quad p > 0$$

which guarantees a finite time reaching phase. The time for moving initial state of the wheelchair to the switching manifold can be expressed as:

$$t = \frac{1}{p} \cdot \ln\left(\frac{p\|s\|_\infty + q}{q} \right). \qquad (22)$$

By adding the proportional rate term ps, the state is forced to reach faster the switching manifold vector

$$s = \begin{bmatrix} s_1 \\ s_2 \end{bmatrix} = \begin{bmatrix} \dot{L}_{h_e} + k_{L_h} L_{h_e} \\ \dot{\phi}_e + k_\phi + k_0 sign(\phi_e)|\theta_e| \end{bmatrix}, \qquad (23)$$

where: k_0, k_{L_h} and k_ϕ are positive constant, $\dot{L}_{h_e}$ and $\dot{\phi}_e$ are defined by (18), (19) and (20). The system (21) can be rewritten as:

$$s = \dot{e} + E, \qquad (24)$$

where

$$E = \begin{bmatrix} E_1 \\ E_2 \end{bmatrix} = \begin{bmatrix} k_{L_h} L_{h_e} \\ k_\phi + k_0 sign(\phi_e)|\theta_e| \end{bmatrix}. \qquad (25)$$

If s_1 converge to zero, trivially $\dot{L}_{h_e}$ converge to zero. If s_2 converge to zero in steady-state, $\dot{\phi}_e$ becomes

$$\dot{\phi}_e = -k_\phi - k_0 sign(\phi_e)|\theta_e| \qquad (26)$$

Since $|\theta_e|$ is always bounded the following relationship between ϕ_e and $\dot{\phi}_e$ holds: If $\phi_e < 0$ then $\dot{\phi}_e > 0$. If $\phi_e > 0$ then $\dot{\phi}_e < 0$. From the time derivative of (24) and using the reaching control input defined in (21), with (18), it obtains after some manipulations:

$$\dot{s} = \ddot{e} + \dot{E} = u_{fosm}, \qquad u_{sm} = \begin{bmatrix} u_{fosm1} \\ ufo_{sm2} \end{bmatrix}, \qquad (27)$$

$$\dot{\upsilon}_c = \frac{u_{fosm1} - E_1 - C_1}{\cos(\gamma_e)}$$
$$\dot{\omega}_c = \frac{u_{sosm2} - E_2 - C_2}{d \cdot \cos(\gamma_e)}, \qquad (28)$$

where:

$$C_1 = \dot{\upsilon}_d \cos(\phi_e + \phi_d) + \upsilon_d \dot{\phi} \sin(\phi_e + \phi_d) + d\dot{\omega}_r \sin(\gamma_e) - (\dot{\theta}_e + \dot{\phi})(\upsilon_r \sin(\gamma_e) - d\omega_r \cos(\gamma_e))$$
$$C_2 = (Lh)^{-1} \begin{bmatrix} \dot{\upsilon}_d \sin(\phi_e + \phi_d) + \upsilon_d \dot{\phi} \cos(\phi_e + \phi_d) - \\ \dot{\upsilon}_r \sin(\gamma_e) - (\dot{\theta}_e + \dot{\phi}) \begin{pmatrix} \upsilon_r \cos(\gamma_e) + \\ d\omega_r \sin(\gamma_e) \end{pmatrix} \end{bmatrix} - \dot{\omega}_d \qquad (29)$$

The control input is transformed in wheel velocities for the right and left wheel, respectively

$$\begin{bmatrix} \omega_R \\ \omega_L \end{bmatrix} = \begin{bmatrix} 1/r & L/r \\ 1/r & -L/r \end{bmatrix} \begin{bmatrix} \upsilon_c \\ \omega_c \end{bmatrix} \qquad (30)$$

As can be observed from equations (27) to calculate the control laws is necessary to know the desired accelerations, $\dot{\upsilon}_d$, $\dot{\omega}_d$ and also the real accelerations of mobile robot, $\dot{\upsilon}_r$, $\dot{\omega}_r$. The linear and angular accelerations could be resulted as derivatives of the corresponding linear and angular speed, but this is undesired due to the noise that lead to the cumulative errors.

To overcome this inconvenience, the trajectory-tracking second-order sliding mode control (TT-SOSMC) was used. SOSMC which is a unique absolutely continuous sliding-mode algorithm, ensuring all the main properties of first order sliding-mode control for the systems with Lipschitz matched uncertainties with bounded gradients and eliminates the chattering phenomenon.

The proposed control input law can be expressed as

$$u_c(t) = [B(e,t)]^{-1} / (u_{sosm}(t) - k_e e(t) - A(e,t)), \qquad (31)$$

where the super twisting controller is:

$$u_{sosm}(t) = -k_1 \operatorname{sgn}(s(t)) \sqrt{|s(t)|} - k_2 s(t) + \sigma(t). \qquad (32)$$

Variations of the term σ are described by:

$$\dot{\sigma}(t) = -k_3 \operatorname{sgn}(s(t)) - k_4 s(t), \qquad (33)$$

where: k_1, k_2, k_3, k_4 are positive scalar constants, and $s = [s_1 \quad s_2]^T$.

To make the discontinuous control input in a continuous one an integrator is added into the control loop. Therefore, the derivative of the sliding surface vector is:

$$\dot{s} = \begin{bmatrix} \dot{s}_1 \\ \dot{s}_2 \end{bmatrix} = \begin{bmatrix} \dot{L}_{h_e} + k_{L_h} L_{h_e} \\ \dot{\phi}_e + k_\phi + k_0 sign(\phi_e)|\theta_e| \end{bmatrix}, \quad (34)$$

which can be expressed as:

$$\dot{s} = \dot{e} + E\,. \quad (35)$$

In eq. (34) is easy to see that the sliding surface in SOSMC is the integral of the sliding surface used in FOSMC.

$$s(t) = e(t) + k_e \int_0^t e(\tau) d\tau \quad (36)$$

This has the effect of eliminating the integration step in the calculus of the control input vector for the SOSMC algorithm. For the stability proof, it is chosen as Lyapunov function candidate, [3], [4]:

$$V = 2k_3|s| + k_4 s^T \cdot s + \frac{1}{2}\sigma^T\sigma + \zeta^T\zeta \quad (37)$$

where

$$\zeta = k_1 sign(s)|s|^{1/2} + k_2 s - \sigma \quad (38)$$

The derivative of Lyapunov function is negative semi-definite, $\dot{V} \le 0$, if the following conditions are satisfied:

$$k_1^2 = \frac{5}{8}k_3,\ k_2^2 = 2k_4 \quad (39)$$

Computing (31), the expressions for linear and angular velocity are the following

$$\upsilon_c = \frac{B_{22}[u_{sosm1} - E_1 - A_1] - B_{12}[u_{sosm2} - E_2 - A_2]}{B_{11}B_{22} - B_{12}B_{21}} \quad (40)$$

$$\omega_c = \frac{B_{11}[u_{sosm2} - E_2 - A_2] - B_{21}[u_{sosm1} - E_1 - A_1]}{B_{11}B_{22} - B_{12}B_{21}} \quad (41)$$

where A_i, B_{ij}, E_i are the elements of the matrix B and vectors A and E defined through the equations (19), (20) and (25).

VI. Closed Loop Real-Time Control

The proposed TT-SOSMC of the CPW, written in visual C++, was implemented in real-time with a sample time $T_s = 100ms$ on an embedded PC. Optical encoders are installed on the driving motor axes. The encoder reading is used to measure the CPW speeds, the CPW position and orientation (by fusing the encoder reading with the gyro measurement). In Fig. 6 and Fig. 7, is easy to observe that the CPW moves along the trajectory and the CPW's real-time trajectory is very close to the desired trajectory. During this movement, the CPW keeps the desired distance ($L_{h_d} = 0.3m$) and desired angle ($\phi_d = -135^\circ$) to the median axis of the path. In Fig. 8, the desired linear and angular speeds are presented. Fig. 9 and Fig.10 show the evolution of the linear and angular speeds, both for the control input and the controlled output of the wheelchair. One can observe that the largest differences between the control input velocities and those of the wheelchair to the first seconds of the real-time control.

Figure 6. Real-time control of CPW

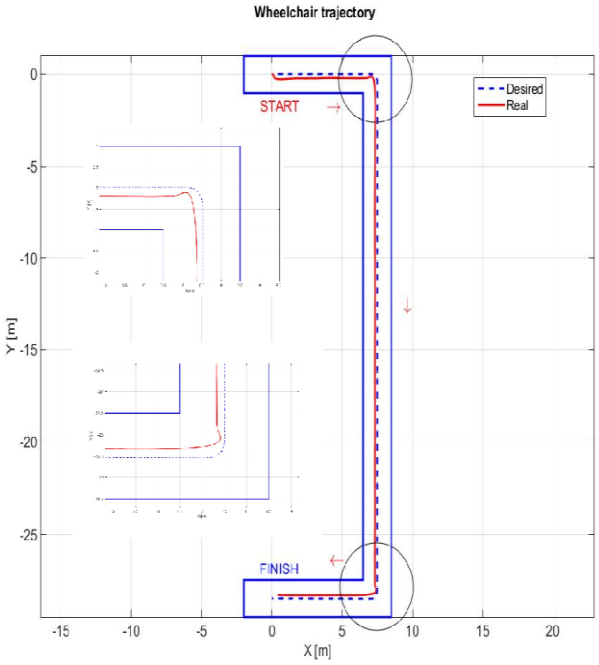

Figure 7. Desired and real-time trajectories

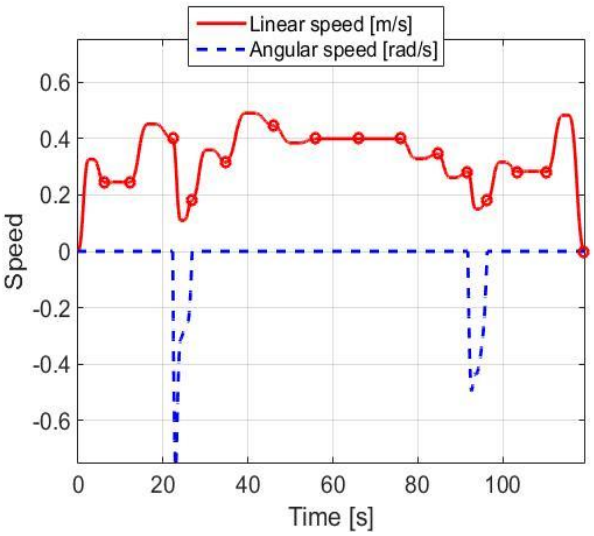

Figure 8. Desired linear and angular speeds

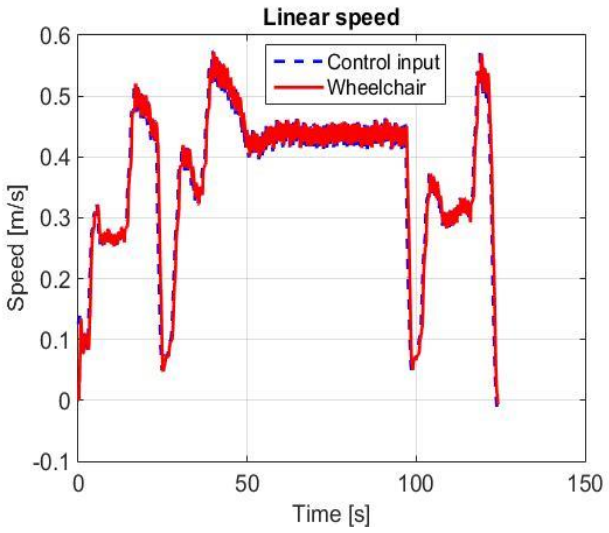

Figure 9. Real-time control input and controlled output linear speed

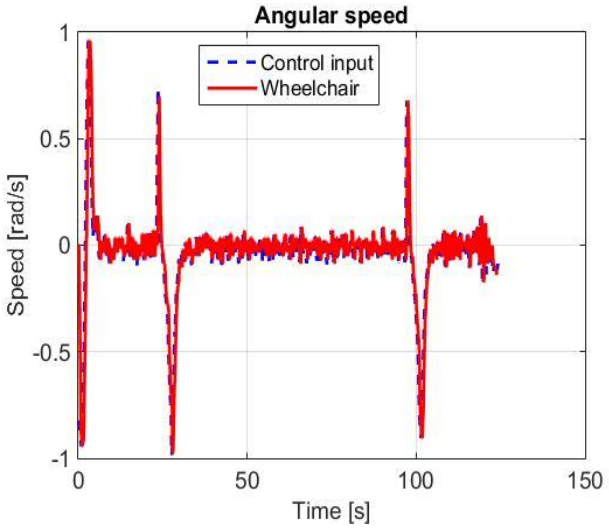

Figure 10. Real-time control input and controlled output angular speed

VII. CONCLUSIONS

This paper mainly deals a kinematic model based trajectory-tracking second-order sliding-mode controller applied to a wheelchair like as a WMR with 2DW/2FW. The SOSMC is a super-twisting control type that is able to alleviate or to eliminate the chattering, improving the tracking performance and robustness. The proposed TT-SOSMC was easy implemented in real-time on CPW. Using a C++ platform, the controller was tested via simulation and real-time on a wheelchair fully equipped for autonomous displacement and navigation. The main conclusion after tests was the differences between the linear and angular speeds between simulation and real-time. The differences are due to the inertia, friction and slippage of the CPW to real-time control, especially at straight angels ($\theta_d = 90^\circ$). Simulated and real-time driving has been tested on a desired trajectory that has multiple straight angles It is known that classical trajectory tracking control algorithms generate high tracking errors for such turns. As future research and testing with fully-equipped CPW will consist of implementation of some navigation methods for fixed and mobile obstacle avoidance methods based on laser and video-biometry of the face and eyeball movements. All this makes the CPW also address people with severe neuro-motor disabilities.

ACKNOWLEDGMENT

This work was supported by UEFISCDI, project numbers PN-III-P1-1.2-PCCDI-2017-0290, project title: *Intelligent and distributed control of 3 complex autonomous systems integrated into emerging technologies for medical-social personal assistance and servicing of precision flexible manufacturing lines.*

REFERENCES

[1] A. Polyakov and A. Poznyak, Reaching Time Estimation for Super Twisting Second Order Sliding Mode Controller via Lyapunov Function Designing, IEEE Transactions on Automatic Control, Vol. 54(8), pp. 1951-1955, 2009.

[2] A. Levant, Higher-Order Sliding Modes, Differentiation and Output Feedback Control, International Journal of Control, Vol. 76(9-10), pp. 924941, 2003.

[3] [J. A. Moreno and M. Osorio. Strict Lyapunov Functions for the Super Twisting Algorithm, IEEE Transactions on Automatic Control, Vol. 57(4), pp. 10351040, 2012.

[4] 1J.A. Moreno, M. Osorio, A Lyapunov approach to second-order sliding mode controllers and observers, Proceedings of 47th IEEE Conference on Decision and Control (CDC 2008), pp. 2856-2861, 2008.

[5] I. Nagesha and C. Edwardsb, Technical Communication: A Multivariable Super-twisting Sliding Mode Approach, Journal Automatica (Journal of IFAC), Vol. 50(3), pp. 984-988, 2014.

[6] R. Solea, A. Filipescu, A. Filipescu Jr. E. Minca, S. Filipescu, Wheelchair Control and Navigation Based on Kinematic Model and Iris Movement, Proceedings of the 2015 7th IEEE International Conference on Robotics,Automation and Mechatronics (CIS&RAM), 15 – 17 July 2015, Angkor Wat, Cambodia, IEEE Catalog Number: CFP15835-CDR, ISBN: 978-1-4673-7336-4, pp:78-83.

[7] R. Solea and D. Cernega, Super Twisting Sliding Mode Controller Applied to a Nonholonomic Mobile RobotProceedings of the 19th IEEE, International Conference on System Theory, Control and Computing, ICSTCC2015 14-16, Oct. 2015, Cheile Gradistei, Romania, pp. 87-92,ISBN: 978-1-4799-8481-7/15/$31.00 ©2015 IEEE

[8] Gonzalez, T., Moreno, J.A., and Fridman, L. (2012). Variable gain super-twisting sliding-mode control. *IEEE Tran. on Automatic Control*, 57(8), 2100-2105.

[9] http://www.mobilerobots.com/software/mobilesim.aspx.

[10] https://www.visualstudio.com/vs/cplusplus